THE JOURNAL OF BIOLOGICAL CHEMISTRY

Vol. 269, No. 44, Issue of November 4, pp. 27409–27413, 1994
Printed in U.S.A.

Tertiary Conformational Changes of the *Neurospora crassa* Plasma Membrane H⁺-ATPase Monitored by Hydrogen/Deuterium Exchange Kinetics

A FOURIER TRANSFORM INFRARED SPECTROSCOPY APPROACH*

(Received for publication, June 9, 1994, and in revised form, August 24, 1994)

Erik Goormaghtigh‡§, Laurence Vigneron‡¶, Gene A. Scarborough‖, and Jean-Marie Ruysschaert‡

From the Laboratoire de Chimie Physique des Macromolécules aux Interfaces, Université Libre de Bruxelles, CP 206/2, Bd du Triomphe, B-1050 Bruxelles, Belgium and the ‖Department of Pharmacology, School of Medicine, University of North Carolina at Chapel Hill, Chapel Hill, North Carolina 27514

Attenuated total reflection Fourier transform infrared spectroscopy of hydrated films of the *Neurospora crassa* plasma membrane H⁺-ATPase has been used to monitor the α-helix and β-sheet contents and amide hydrogen exchange rates of the enzyme in the absence of ligands or locked in several stages of the enzyme catalytic cycle by MgADP, Mg-vanadate, and MgATP-vanadate. No difference larger than 2% was found in the α-helix or β-sheet content of the H⁺-ATPase in different conformational states. However, when the rate of hydrogen/deuterium exchange monitored by the evolution of the area of amide II and amide II′ is decomposed into three components, the number of amide protons characterized by a short exchange rate (1.1 min) falls from 38% of the protein amide protons (or 37% in the presence of Mg^{2+} alone) to 24–27% in the presence of Mg-vanadate and MgATP-vanadate and to 19% in the presence of MgADP. These results suggest that the conformational changes known to occur when the H⁺-ATPase interacts with the above ligands are predominantly tertiary structure changes.

The P-type ATPases form a family of ATPases constituted of one or two polypeptide chains and use the free energy of ATP to generate ion gradients across a variety of different biological membranes. Prominent members of this class of transporter are the Ca^{2+}-ATPase from sarcoplasmic reticulum, the H^+/K^+-ATPase from the gastric mucosa, the Na^+/K^+-ATPase of animal plasma membranes and H⁺-ATPases from fungal plasma membranes. All of these enzymes share a common molecular mechanism which involves a phosphorylated intermediate, and all are inhibited by vanadate at μM concentrations. Even though a number of intermediates of the catalytic cycle can be recognized by indirect approaches, little is known about the structure of these proteins at the different stages of their catalytic cycles. The neurospora enzyme is a particularly simple P-type ATPase, since its activity is contained in a single polypeptide chain (Scarborough and Addison, 1984) and since monomers catalyze both ATP hydrolysis and proton pumping (Goormaghtigh *et al.*, 1986). Conformational changes in the enzyme structure have been detected by limited trypsinolysis experiments (Addison and Scarborough, 1982). In the absence of ligands or in the presence of Mg^{2+}, the enzyme is rapidly degraded into small pieces. In the presence of MgATP-vanadate or Mg-vanadate, trypsinolysis produces two remarkably stable peptides of apparent M_r ~95,000 and 88,000. In the presence of MgADP, only the M_r ~88,000 peptide is observed. The exact localization of the trypsin sites at the N terminus has been determined by Mandala and Slayman (1988). A description at the molecular level of the conformational changes indicated by these limited proteolysis experiments is, however, still missing. We show in the present communication that Fourier transform infrared spectroscopy (FTIR)[1] is a useful tool for obtaining quantitative data about the secondary and tertiary structure of the *Neurospora crassa* H⁺-ATPase molecule locked into several different conformations by specific ligands.

EXPERIMENTAL PROCEDURES

H⁺-ATPase Isolation—The *N. crassa* plasma membrane H⁺-ATPase was isolated by the large scale procedure as described previously (Smith and Scarborough, 1984; Scarborough 1988). The purified ATPase was placed in a 0.5 mM phosphate buffer (pH 6.8), containing various amounts of lyso-PG by running 350 μg of the purified ATPase (1 ml) on a Sephadex G-50 (Pharmacia) column (1 × 25 cm) equilibrated with this buffer at 1 ml/min at room temperature (20 °C). The fractions containing about 90% of the ATPase were concentrated to approximately 5 mg/ml using RCF-ConFilt-hollow fiber bundles (M_r cutoff 6000; Bio-Molecular Dynamics). ATPase activity was assayed in a medium containing the following constituents: 4 μl of 0.1 M EDTA (pH 6.8 with Tris), 10 μl of 0.1 M NaN_3, 10 μl of 200 mM MgATP (pH 6.8 with Tris), 8 μl 0.5 M $(NH_4)_2SO_4$, 58 μl of 0.1 M Mes-Tris (pH 6.8), and either 10 μl of 5 mg/ml bovine brain extract (Folch fraction I) (Scarborough and Addison, 1984) or 10 μl of water. Reactions were initiated by addition of approximately 1 μg of protein and allowed to proceed for 5 min at 30 °C. They were stopped by addition of 100 μl of 5% SDS. Inorganic phosphate released was estimated as described before for this enzyme (Scarborough, 1988). Protein concentration was determined by the method of Lowry *et al.* (1951) as modified by Bensadoun and Weinstein (1976).

Infrared Spectroscopy—Attenuated total reflection infrared (ATR-FTIR) spectra were obtained on a Perkin-Elmer 1720X FTIR spectrophotometer equipped with a liquid nitrogen cooled mercury cadmium telluride detector at a resolution of 4 cm^{-1}. 256 scans were averaged for each measurement. After every four scans, reference spectra of a clean germanium plate were automatically recorded by a sample shuttle accessory and ratioed against the recently run sample spectra. The spec-

* This work was supported by the Action de Recherche Concertée, Belgium and by United States Public Health Service National Institutes of Health Grant GM24784. The costs of publication of this article were defrayed in part by the payment of page charges. This article must therefore be hereby marked "*advertisement*" in accordance with 18 U.S.C. Section 1734 solely to indicate this fact.

§ Research Associate of the National Fund for Scientific Research (Belgium). To whom correspondence should be addressed: ULB Campus Plaine C.P. 206/2, B-1050 Brussels Belgium. Tel: 32-2-650-53-86; Fax: 32-2-650-51-13.

¶ I.R.S.I.A. fellow (Belgium).

[1] The abbreviations used are: FTIR, Fourier transform infrared spectroscopy; ATR, attenuated total reflection; H/D: hydrogen/deuterium; lyso-PG, lysophosphatidylglycerol.

trophotometer was continuously purged with dry air. The internal reflection element was a germanium ATR plate (50 × 20 × 2 mm, Harrick EJ2121) with an aperture angle of 45°, yielding 25 internal reflections. Measurements were carried out at 20 °C. Thin films were obtained by slowly evaporating a sample containing 50 μg of protein on one side of the ATR plate under a stream of nitrogen (Fringeli and Günthard, 1981; Goormaghtigh and Ruysschaert, 1990). The ATR plate was then sealed in a universal sample holder (Perkin-Elmer) and deuterated by flushing the sample compartment with D_2O-saturated N_2 (room temperature) for 3 h. Determination of the protein secondary structure by analysis of the shape of the deuterated amide band has been described previously (Cabiaux *et al.*, 1989; Goormaghtigh *et al.*, 1990).

Hydrogen/Deuterium Exchange—Films containing 50 μg of protein were prepared on a germanium plate as described above. Nitrogen gas was saturated with D_2O by bubbling through a series of five vials containing D_2O. In each vial, the nitrogen was passed through a Millipore 0.8-μm filter wetted with D_2O. The flow rate of 75 ml/min was controlled by a Brooks flow meter. Bubbling was started at least 1 h before starting the experiments. At the zero time, the tubing was connected to the cavity of the sealed chamber surrounding the film. 12 spectra were recorded and averaged at a resolution of 4 cm^{-1} for each kinetic time point. A computer program was written to drive the spectrophotometer during the kinetics measurements. At the beginning of the kinetics measurements, spectra were recorded every 15 s. After the first 2 min, the time interval was logarithmically increased. After 16 min, the interval between the scans was large enough to allow the interdigitation of a second kinetics measurement. A second sample placed on another ATR setup of the Perkin-Elmer sample shuttle was then analyzed with the same time sampling with a 16-min offset by connecting the D_20-saturated N_2 flow in series with the first sample. From this time on, our program changed the shuttle position to follow both kinetics measurements. Before starting the deuteration, 10 spectra of each sample were recorded in order to test the stability of the measurements and the reproducibility of area determination. Usually, one of the samples placed on the shuttle was prepared in the absence of ligands and the other was prepared in the presence of a ligand as indicated. This procedure allowed us to test the reproducibility of the experiment under identical conditions. A background deuteration kinetics measurement recorded with the same germanium plate at the same position in the sample shuttle but in the absence of sample was recorded and subtracted from the data recorded in the presence of the sample. This allowed us to take into account the unavoidable variations in the atmospheric water content inside of the spectrophotometer. The subtraction of the background kinetics measurement was made more accurate by adopting the following automated procedure: a subtraction coefficient was first computed as the ratio of the area of the atmospheric water band integrated between 1565 and 1551 cm^{-1} on the sample spectrum and on the corresponding background spectrum. The subtraction coefficients obtained for each kinetic time point were then plotted against the time and the resulting curve was fitted with a 4th order polynomial. Values of the subtraction coefficients obtained from the polynomial were finally used. The areas of amides I, II, and II′ were obtained by integration between 1702–1596, 1596–1502, and 1492–1412, respectively. For each spectrum, the area of amide II and amide II′ was divided by the area of amide I. This allowed us to take into account small but significant variations of the overall spectral intensity due in part to the presence of D_2O which induces minor swelling of the sample layer and therefore increases the average distance between the protein sample and the germanium interface. Since the ATR spectrum intensity depends on this distance (Harrick, 1967), this results in a loss of a few percent of the band intensity for all measured bands. Undeuterated spectra were recorded before the kinetics measurement experiments as explained above, and 100% deuterated samples were obtained after the experiments by placing the samples in 50-ml capped tubes containing 2 ml of D_2O at 100 °C for 30 min. In such conditions, the intensity of amide II fell from 47% of the intensity of amide I to 2% of the intensity of amide I (not shown). This is in agreement with the weak contribution of amino acid side chains in the amide I and amide II region that we have described elsewhere (Goormaghtigh *et al.*, 1994). The area of amide II and II′ (relative to the area of amide I) was finally expressed between 0 and 100% for each kinetic time point.

Materials—Vanadate-free ATP, ADP, lyso-PG, and bovine trypsin inhibitor were from Sigma, and D_2O was from Merck (Germany). Distilled water was used throughout the experiments. All other reagents were of the highest purity available.

RESULTS

We have shown previously that the lyso-PG·ATPase complex is a hexameric assembly of active ATPase monomers which is water-soluble (Chadwick *et al.*, 1987; Hennessey and Scarborough, 1988). In a first step we determined the concentration of lyso-PG which best activates ATP hydrolysis. This was found to be 5 μg/ml of free lyso-PG which is best obtained by running the purified ATPase on a Sephadex G50 column equilibrated with this lyso-PG concentration, as described under "Experimental Procedures." At this optimal lyso-PG concentration, the specific activity of the ATPase is 20 μmol of ATP hydrolyzed/min/mg of protein. The Fourier transform ATR infrared experiments involve the formation of a film by gentle drying of the sample on a germanium crystal under a stream of nitrogen. In order to mimic these conditions, we prepared films of the lyso-PG·ATPase in glass test tubes which were incubated for different period of time at room temperature. Importantly, we found that the specific activity of the lyso-PG·ATPase contained in films incubated for up to 120 min was not altered by this treatment after rehydration in aqueous buffer. We also established that the lyso-PG·ATPase can be frozen in liquid nitrogen and kept at −20 °C for weeks without loss of activity. This property allowed us to perform numerous experiments with the same stock solution of lyso-PG·ATPase.

IR-ATR spectra of the lyso-PG·ATPase recorded in the absence and in the presence of ligands known to induce ATPase conformational changes are reported in Fig. 1. Full access of the ligands to all the ATPase molecules is obtained by forming the film in the presence of the ligands. The two main bands located around 1654 and 1544 cm^{-1} are assigned to the amide I and amide II vibrations of the protein. The weak band at 1732 cm^{-1} is assigned to the ester ν(C=O) from the lyso-PG. The position of amide I at 1654 cm^{-1} indicates a relatively high amount of α-helix in the protein and the low frequency shoulder near 1632 cm^{-1} indicates the presence of significant amount of β-sheet (Byler and Susi, 1986; Goormaghtigh *et al.*, 1994). For the sake of the comparison, the spectra of the predominantly α-helix-containing protein bacteriorhodopsin (Henderson *at al.*, 1990) reconstituted in L-α-dimyristoylphosphatidylcholine vesicles (amide I at 1658 cm^{-1} and amide II at 1543 cm^{-1}) and of the predominantly β-sheet *Escherichia coli* porin (Cowan *et al.*, 1992) reconstituted in L-α-dimyristoylphosphatidylcholine vesicles (amide I at 1629 cm^{-1} and amide II at 1526 cm^{-1}) are reported on the same figure. The shape of amide I for the undeuterated lyso-PG-ATPase in the absence and presence of the various ligands is very similar. The secondary structure of the lyso-PG-ATPase was analyzed from the shape of amide I of deuterated samples after Fourier self-deconvolution and curve fitting as detailed in Goormaghtigh *et al.* (1990). Spectra were recorded in the absence of ligands and in the presence of the following species: Mg^{2+}, Mg^{2+}-vanadate, MgATP-vanadate, MgADP (concentrations as in Fig. 1). The secondary structure is reported in Table I for the ligands tested. Clearly, the secondary structure of the ATPase changes little upon binding of the various ligands.

Since the secondary structure of the protein undergoes little modification in the presence of the various ligands known to lock the enzyme in different structures as indicated by its sensitivity to proteolysis, it is probable that the tertiary structure changes of the protein are responsible for the observed differences in proteolytic sensitivity (Addison and Scarborough, 1982). For a near-constant secondary structure and other constant experimental conditions, including pH and temperature, the rate of H/D exchange can be used as an indicator of tertiary structure changes. A series of spectra recorded as a function of the deuteration time in the absence of ligands appears in

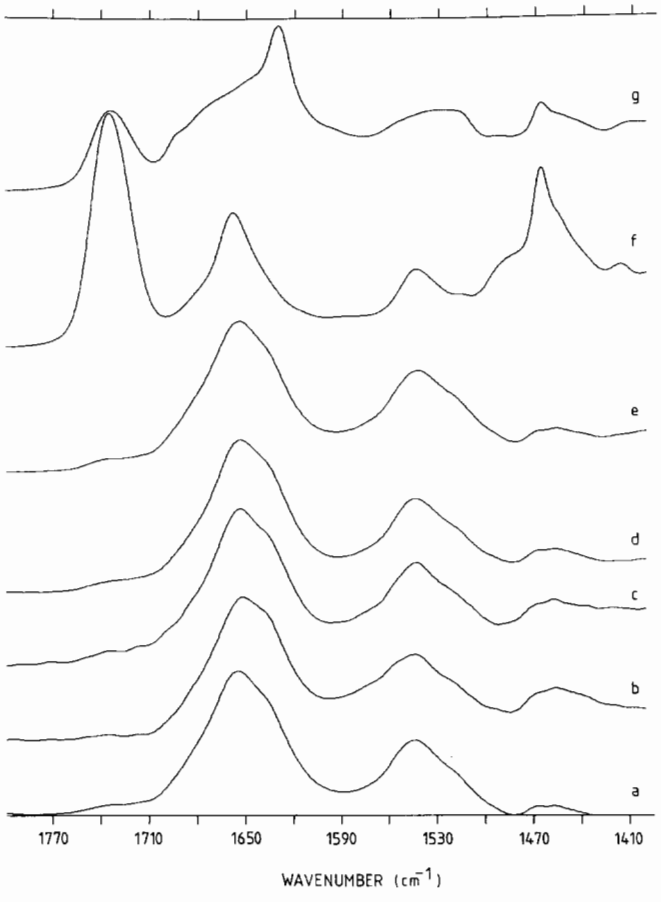

FIG. 1. **Infrared spectra between 1800 and 1400 cm^{-1} of the *N. crassa* plasma membrane H$^+$-ATPase and two reference proteins.** 20 µl containing 50–100 µg of ATPase in a 0.5 mM phosphate buffer (pH 6.8) containing 5 µg/ml of lyso-PG and the various ligands were used to form films as described under "Experimental Procedures." *Spectrum a*, no ligand added; *spectrum b*, 10 mM $MgSO_4$; *spectrum c*, 10 mM $MgSO_4$, 0.1 mM vanadate; *spectrum d*, 2 mM MgATP, 0.1 mM vanadate (sodium salt); *spectrum e*, 2 mM MgADP. *Spectra f* and *g* are, respectively, the spectra of bacteriorhodopsin and *E. coli* porin reconstituted in L-α-dimyristoylphosphatidylcholine vesicles as described in (Goormaghtigh *et al.*, 1990). Spectra have been rescaled to the same amplitude and offset.

TABLE I
Secondary structure of the N. crassa plasma membrane ATPase determined in the presence of different ligands (see Fig. 1) by analysis of the shape of the amide I band according to Goomaghtigh et al. (1990)

	α-Helix	β-Sheet	Turns	Random coil
	%	%	%	%
No ligand	39	30	16	14
$MgSO_4$	37	32	16	14
$MgSO_4$-vanadate	38	31	18	13
MgATP-vanadate	40	32	15	13
MgADP	38	32	15	14

Fig. 2. Clearly the amide II area (near 1550 cm^{-1}) decreases as a function of time and the amide II′ area increases. The decreasing area of amide II (near 1550 cm^{-1}) and the increasing area of amide II′ (near 1450 cm^{-1}) computed between 0 and 100% as explained under "Experimental Procedures" is reported in Fig. 3 for samples prepared in the absence or presence of different ligands. It immediately appears from Fig. 3 that the exchange is faster in the absence of ligands or in the presence of $MgSO_4$ than in the presence of MgATP-vanadate, $MgSO_4$-vanadate, and MgADP. Since the H/D exchange is a first order reaction, the fraction of residual amide protons $H(t)$ is expected

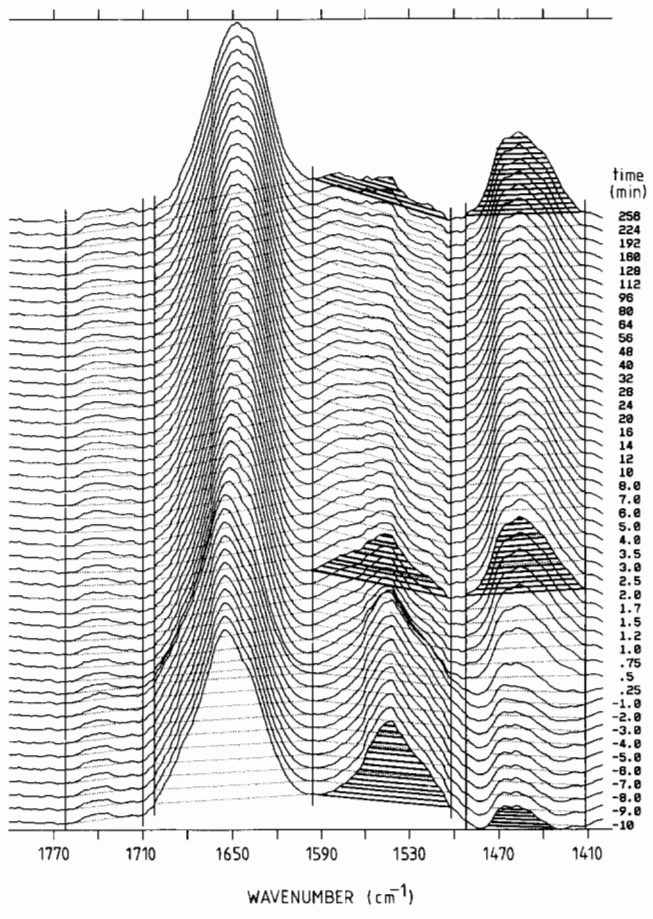

FIG. 2. **Infrared spectra between 1800 and 1400 cm^{-1} of the *N. crassa* plasma membrane H$^+$-ATPase in a 0.5 mM phosphate buffer containing 5 µg/ml of lyso-PG at pH 6.8 in the absence of ligands.** Spectra were recorded as a function of the time of exposure to D_2O-saturated N_2 which is indicated (in minutes) in the *right margin* of the figure. Negative times refer to spectra recorded before starting the deuteration procedure. Integration of the area of amide I, amide II, and amide II′ was performed using the base lines indicated by the *dotted lines* drawn between the intersection of the spectra with the *vertical lines* (see "Experimental Procedures").

to display a multiexponential decay corresponding to the different groups, i, of amides characterized by a common period T_i,

$$H(t) = \sum_i a_i \exp(-t/T_i) \qquad \text{(Eq. 1)}$$

where a_i is the proportion of the group i. A nonlinear fitting of all the curves of Fig. 3 without constraints by Equation 1 for i = 1–3 yields three periods T_1, T_2, and T_3. Since the periods T_1, T_2, and T_3 were similar for all the kinetics curves analyzed, their average values were computed and found to be 1.1 ± 0.8 min, 8.4 ± 3 min, and 368 ± 155 min, respectively. In order to compare the proportions a_i of each amide group for the different curves for identical T_i values, a second fitting was performed with setting the T_i to their average value determined above. Results of this analysis are reported in Table II. No change larger than 2% appeared in these proportions when the periods were set to their average value, indicating the general validity of the average T_i values used for the comparison.

DISCUSSION

The profound effects of several ATPase substrates and transition state analogues on the susceptibility of the H$^+$-ATPase to degradation by trypsin were reported in a previous communication (Addison and Scarborough, 1982). These results were

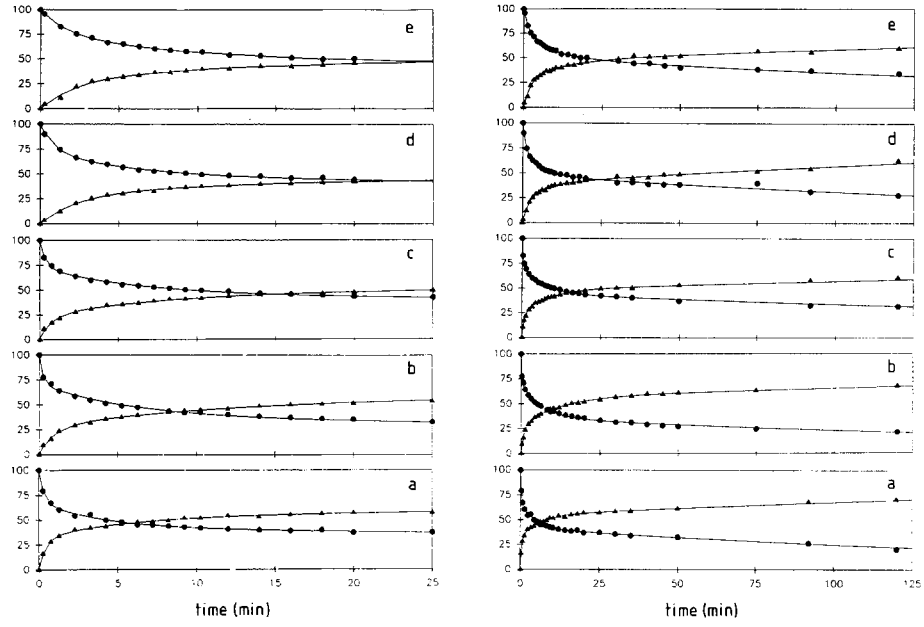

FIG. 3. **Percentage of the maximum area of amide II (●) and amide II′ (▲) reported as a function of the deuteration time for the *N. crassa* plasma membrane H⁺-ATPase in a 0.5 mM phosphate buffer containing 5 μg/ml of lyso-PG at pH 6.8.** *a*, no ligand added; *b*, 10 mM $MgSO_4$; *c*, 10 mM $MgSO_4$, 0.1 mM vanadate; *d*, 2 mM MgATP, 0.1 mM vanadate; *e*, 2 mM MgADP. *Left panel*, reported between 0 and 25 min. *Right panel*, reported between 0 and 125 min.

TABLE II

Proportion a_1, a_2, and a_3 in the exchange kinetic curve recorded in the presence of different ligands (see Fig. 1) of three exponential components characterized by a half-decay of T_1 = 1.1, T_2 = 8.4 and T_3 = 368 min

Numbers in parentheses are the number of amino acid residues involved.

	a_1	a_2	a_3
	%	%	%
No ligand	38 (350)	19 (175)	43 (395)
$MgSO_4$	37 (340)	21 (193)	42 (386)
$MgSO_4$-vanadate	27 (248)	20 (184)	52 (478)
MgATP-vanadate	24 (221)	25 (230)	51 (469)
MgADP	19 (175)	30 (276)	51 (469)

interpreted to indicate that upon binding of MgADP, the ATPase assumes its substrate binding conformation and upon binding MgATP plus vanadate or Mg^{2+} plus vanadate alone, it is locked in a conformation similar to that it assumes during the transition state of the enzyme dephosphorylation reaction (Addison and Scarborough, 1982; Scarborough, 1992). Both the shape of the amide I peak which is conformation-sensitive (Fig. 1) and further analysis of its shape by Fourier self-deconvolution and curve fitting (Table I) indicate that the secondary structure of the H⁺-ATPase is not significantly affected by the presence of these ligands. A similar conclusion has been reached on the basis of our circular dichroism investigation (Hennessey and Scarborough, 1990). Other P-type ATPases have been shown not to be affected in their secondary structure by a variety of ligands (Csermely *et al.*, 1987) or only to a very small extent (Arrondo *et al.*, 1987; Barth *et al.*, 1991; Buchet *et al.*, 1991). FTIR, as used here, has been claimed to be less prone to artifacts in this regard than CD (compare Gresalfi and Wallace (1984) with Chetverin and Brazhnikov (1985)). It should be added that the secondary structure analysis used in the present study does not significantly depend on the degree of H/D exchange extent as soon as the fast exchanging protons belonging mainly to loops and random coil structures have been exchanged. From an analysis of the spectra obtained after different deuteration times (not shown), it appears that the final secondary structure is reached (within less than 1%) after 2 min of deuteration, in agreement with previous observations (Goormaghtigh *et al.*, 1993). Finally, we must mention that from the present data, compensatory changes in the secondary structure cannot be ruled out but seem far less likely. We therefore suggest that the predominant structural changes that occur in the ATPase molecule as it proceeds through its catalytic cycle are tertiary in nature.

Hydrogen isotope exchange has long been used for the analysis of protein structure and dynamics (for reviews, see Englander and Kallenbach (1984) and Kim (1986)). It identifies submolecular motional domains, including fast exchanging protons of the protein surface, somewhat slower exchanging protons of the flexible (loop) regions buried in the protein, slow exchanging protons involved in secondary structures (exchange rate depends on accessibility to the solvent), and the slowly exchanging protons from the protein core formed by the most rigid clusters of amino acids. This slowly exchanging core has been related for several proteins to the initial folding core during the sequence of events leading to the protein folding (Kim *et al.*, 1993).

The interpretation of the H/D exchange kinetics reported here in terms of tertiary structure changes in the H⁺-ATPase requires a careful examination of the data. First, except for differences in the added ligands, all the experimental conditions should be kept constant, including pH, temperature, and the protein secondary structure. As noted above, the secondary structure of the H⁺-ATPase does not change significantly in the presence of the various ligands, but the stability of a number of secondary structures could be affected without gross modification of the structure itself. This would have a significant effect on the exchange rates. However, changes in secondary structure stability involve hydrogen bond modifications and in turn significant spectral changes in the amide I and amide II region (for a review, see Goormaghtigh *et al.* (1994)). Analysis of the FTIR spectra of the H⁺-ATPase indicates that such changes do not take place upon addition of ligands. Another concern in this study was that the ligands might catalyze or nonspecifically slow down the H/D exchange rates. As a control for this, we incubated the bovine pancreatic trypsin inhibitor in the absence of ligands and in the presence of Mg-vanadate as done for the H⁺-ATPase. Since Mg-vanadate is not a specific ligand of bovine trypsin inhibitor, only the non-specific general effects, if any, of this ligand on the exchange rate should appear. The experiment (not shown) indicated clearly that no effect of Mg-vanadate could be measured for bovine trypsin inhibitor. This experiment simultaneously indicates adequate control of the

pH in the films, since the exchange rate is strongly pH-dependent. In another control experiment we added increasing amounts of the ATPase solution to the ATR plate (from 10 to 280 μg of protein) in order to check whether the film thickness could hinder the penetration of D_2O and slow down the exchange kinetics. Analysis of the results indicated that the kinetics recorded with the thicker films were identical to these recorded for thin films. This is in agreement with the diffusion coefficient of water across lipid bilayers which reaches tens of μm/s (Fettiplace and Haydon, 1980; Finkelstein, 1987), *i.e.* more than the film thickness per second. Another question raised by the ATR method is that the protein behavior in a film could be different from the protein behavior in solution. This problem has been addressed quite exhaustively before with regard to the determination of secondary structures on films (Goormaghtigh *et al.*, 1990; Goormaghtigh and Ruysschaert, 1990; Demel *et al.*, 1990; Goormaghtigh *et al.*, 1994) and the validity of hydrated films to analyze protein structure assessed. From these considerations it appears that under the hydration conditions used for protein secondary structure determination, there is at least as much water per protein molecule as in many protein crystals which are clearly acceptable subjects for structure analysis. On the other hand, comparing exchange rates in protein crystals *versus* exchange rates in solution has been a matter of debate. It has been shown using lysozyme that as soon as a single water monolayer can be formed about the protein (hydration level above 0.15 g of water/g of protein), the exchange rate reaches its maximum (Schinkel *et al.*, 1985; Rosenberg, 1986). However, in other cases, exchange in the crystal was slowed down, most probably owing to lattice contacts between proteins rather than because of a lack of D_2O solvent accessibility (reviewed by Englander and Kallenbach (1984)). In the case of a membrane protein, being embedded in a two-dimensional layer is the natural situation, and film formation is not expected to enhance lattice contacts. It must be mentioned that, in the absence of a lipid bilayer, the ATPase molecules cannot adopt a specific orientation with respect to the ATR plate. Finally, it has been shown before that the hexameric structure of the H⁺-ATPase is maintained in the presence or in the absence of different detergents, including lyso-PG, and ligands (Hennessey and Scarborough, 1988; Chadwick *et al.*, 1987). Therefore, no ligand-mediated aggregation is expected to play a role in the exchange kinetics we have observed. It is thus reasonable to conclude that the ligand effects we have observed are related only to the protein tertiary structure.

As summarized in Table II, of about 350 possible fast exchangeable amide protons (in the absence of ligand or in the presence of Mg^{2+} alone), 102 or 129 are protected in the presence of Mg-vanadate or MgATP-vanadate, and 175 are protected in the presence of MgADP. The protected amide protons are changed to medium or slow exchanging species in Table II. These results are quite consistent with the limited trypsin degradation experiments; in the absence of ligands or in the presence of Mg^{2+} alone, the H⁺-ATPase is rapidly degraded into numerous small fragments; in the presence of Mg-vanadate or MgATP-vanadate, an 88-kDa and a 95-kDa peptide are protected; and in the presence of MgADP, a single 88-kDa peptide is protected (Addison and Scarborough, 1982). Clearly a qualitative match exists between the proteolytic and the H/D exchange experiments.

The retardation of exchange is a function of the reactivity of the NH group, partially determined by the involvement of amide hydrogen in hydrogen bonding and, partially due to its accessibility to the solvent. The variations observed in the exchange rate upon addition of ligands could therefore be ascribed to a decrease of the molecular surface in contact with the solvent and/or to a decrease in the molecular fluctuation involving tightening of the molecular architecture (Woodward *et al.*, 1982). This is consistent with the closing of a cleft around the ligands which would subtract a substantial part of the protein surface from access to the aqueous solvent as has been suggested before (Scarborough, 1985, 1992). The opening of the molecular structure and the resulting greater accessibility of the H⁺-ATPase surface area to the solvent in the unliganded enzyme might readily explain the extreme sensitivity of the H⁺-ATPase to tryptic degradation in the absence of ATPase ligands when compared with the liganded structures (Addison and Scarborough, 1982).

In conclusion, the data accumulated in the present communication indicate that the environment of 10–20% of the amino acid residues of the *N. crassa* plasma membrane H⁺-ATPase is modified when the enzyme assumes the substrate binding and transition state conformations it assumes during the catalytic cycle. The secondary structure of the H⁺-ATPase is not significantly affected.

REFERENCES

Addison, R. (1986) *J. Biol. Chem.* **261,** 14896–14901

Addison, R., and Scarborough, G. A. (1982) *J. Biol. Chem.* **257,** 10421–10426

Amory, A., and Goffeau, A. (1982) *J. Biol. Chem.* **257,** 4723–4730

Arrondo, J. L., Mantsch, H. H., Mullner, N., Pikula, S., and Martonosi, A. (1987) *J. Biol. Chem.* **262,** 9037–9043

Barth, A., Mäntele, W., and Kreutz, W. (1991) *Biochim. Biophys. Acta* **1057,** 115–123

Bensadoun, A., and Weinstein, D. (1976) *Anal. Biochem.* **70,** 241–250

Brooker, R. J., and Slmayman, C. W. (1983) *J. Biol. Chem.* **258,** 222–226

Buchet, R. Varga, S., Seidler, N. W., Molnar, E., and Martonosi, A. (1991) *Biochim. Biophys. Acta* **1068,** 201–216

Byler, D. M., and Susi, H. (1986) *Biopolymers* **25,** 469–487

Cabiaux, V., Brasseur, R., Wattiez, R., Falmagne, P., Ruysschaert, J. M., and Goormaghtigh, E. (1989) *J. Biol. Chem.* **264,** 4928–4938

Chadwick, C. C., Goormaghtigh, E., and Scarborough, G. A. (1987) *Arch. Biochem. Biophys.* **252,** 348–356

Chetverin, A. B., and Brazhnikov, E. V. (1985) *J. Biol. Chem.* **260,** 7817–7819

Cowan, S. W., Schirmer, T., Rummel, G., Steiert, M., Ghosh, R., Pauptit, R. A., Jansonius, J. N., and Rosenbusch, J. P. (1992) *Nature* **358,** 727–733

Csermely, P., Katopis, C., Wallace, B., and Martonosi, A. (1987) *Biochem. J.* **241,** 663–669

Demel, R., Goormaghtigh, E., and Ruysschaert, J. M. (1990) *Biochim. Biophys. Acta* **1027,** 155–162

Englander, S. W., and Kallenbach, N. R. (1984) *Q. Rev. Biophys.* **16,** 521–655

Fettiplace, R., and Haydon, D. A. (1980) *Am. Physiol. Soc.* **60,** 510–550

Finkelstein, A. (1987) *Water Movement through Lipid Bilayers, Pores, and Plasma Membrane. Theory and Reality* (Finkelstein, A. J., ed) John Wiley & Sons Inc.

Fringeli, U. P., and Günthard, H. H. (1981) *Mol. Biol. Biochem. Biophys.* **31,** 270–33

Goormaghtigh, E., and Ruysschaert, J. M. (1990) in *Molecular Description of Biological Membrane Components by Computer Aided Conformational Analysis* (Brasseur, R., ed) pp. 285–329, CRC Press, Boca Raton, FL

Goormaghtigh, E., Chadwick, C., and Scarborough, G. A. (1986) *J. Biol. Chem.* **261,** 7466–7471

Goormaghtigh, E., Cabiaux, V., and Ruysschaert, J. M. (1990) *Eur. J. Biochem.* **193,** 409–420

Goormaghtigh, E., Cabiaux, V., De Meutter, J., Rosseneu, M., and Ruysschaert, J. M. (1993) *Biochemistry* **32,** 6104–6110

Goormaghtigh, E., Cabiaux, V., and Ruysschaert, J. M. (1994) *Subcell. Biochem.* **23,** 329–450

Gresalfi, T. J., and Wallace, B. A.(1984) *J. Biol. Chem.* **259,** 2622–2628

Harrick, N. J. (1967) *Internal Reflection Spectroscopy,* J. Wiley & Sons Inc., New York

Henderson, R., Baldwin, J. M., Ceska, T. A., Zemlin, F., Beckmann, E., and Downing, K. H. (1990) *J. Mol. Biol.* **213,** 899–929

Hennessey, J. P., Jr., and Scarborough, G. A. (1988) *J. Biol. Chem.* **263,** 3123–3130

Hennessey, J. P., Jr., and Scarborough, G. A. (1990) *J. Biol. Chem.* **265,** 532–537

Kim, S. K. (1986) *Methods Enzymol.* **131,** 136–157

Kim, K.-S., Fuchs, J. A., and Woodward, C. K. (1993) *Biochemistry* **32,** 9600–9608

Lowry, O. H., Rosebrough, N. J., Farr, A. L., and Randall, R. J. (1951) *J. Biol. Chem.* **193,** 265–275

Mandala, S. M., and Slayman, C. (1988) *J. Biol. Chem.* **263,** 15122–15128

Rosenberg, A. (1986) *Methods. Enzymol.* **127,** 630–648

Scarborough, G. A. (1985) *Microbiol. Rev.* **49,** 214–231

Scarborough, G. A. (1988) *Methods Enzymol.* **157,** 574–579

Scarborough, G. A. (1992) in *Molecular Aspects of Transport Proteins* (De Pont, H. H. M., ed) pp. 117–134, Elsevier Science Publishing Co., Inc., New York

Scarborough, G. A., and Addison, R. (1984) *J. Biol. Chem.* **259,** 9109–9114

Schinkel, J. E., Downer, N. W., and Rupley, J. A. (1985) *Biochemistry* **24,** 352–366

Smith, R., and Scarborough, G. A. (1984) *Anal. Biochem.* **138,** 156–163

Woodward, C. K., Simon, I., and Tuchsen, E. (1982) *Mol. Cell. Biochem.* **48,** 135–160